TG–759
DECEMBER 1965
Copy No. 33

Technical Memorandum

HEAT TRANSFER EFFECTS ARISING FROM ARC ROTATION IN PLASMA ARC HEATERS OF THE SELF-INDUCED MAGNETIC FIELD TYPE

by E. A. BUNT

THE JOHNS HOPKINS UNIVERSITY • APPLIED PHYSICS LABORATORY

DISCLAIMER NOTICE

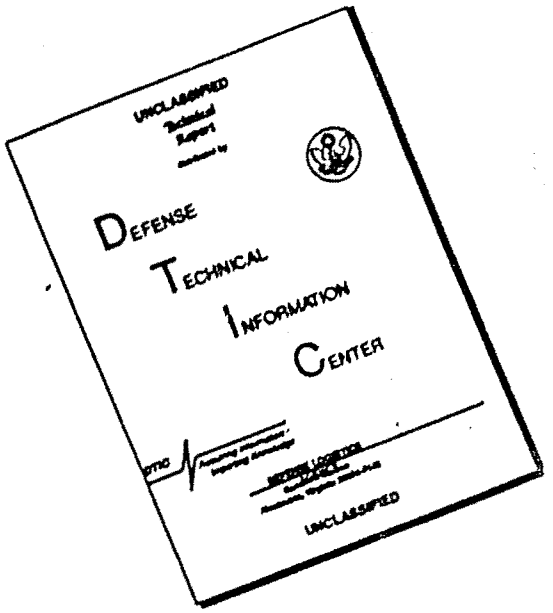

THIS DOCUMENT IS BEST QUALITY AVAILABLE. THE COPY FURNISHED TO DTIC CONTAINED A SIGNIFICANT NUMBER OF PAGES WHICH DO NOT REPRODUCE LEGIBLY.

TG—759
DECEMBER 1965

Technical Memorandum

HEAT TRANSFER EFFECTS ARISING FROM ARC ROTATION IN PLASMA ARC HEATERS OF THE SELF-INDUCED MAGNETIC FIELD TYPE

by E. A. BUNT

THE JOHNS HOPKINS UNIVERSITY ▪ APPLIED PHYSICS LABORATORY
8621 Georgia Avenue, Silver Spring, Maryland 20910

Operating under Contract NOw 62-0604-c, Bureau of Naval Weapons, Department of the Navy

The Johns Hopkins University
APPLIED PHYSICS LABORATORY
Silver Spring, Maryland

SUMMARY

This paper is concerned with an analysis of the thermal behavior of high input power (~15 Megawatt) arc heaters operating at values of total (bulk) enthalpy up to 2500 Btu/lb. Such heaters are currently in use to supply air for aerodynamic testing purposes, including subsonic turbulent pipe flow, the operation of propulsion tunnels with "full" temperature simulation, and supersonic combustion ducts. The electrode system is essentially a "rail accelerator" adapted for continuous operation by making it re-entrant; the self-induced magnetic field brings about rapid movement of the arc roots to prevent destruction of the electrodes. The rate of rotation of the arc column (which is subject to aerodynamic drag) is shown to be a function of apparent electrode gap and current and the stagnation temperature and pressure in the arc chamber. A distinction can also be drawn between "long" and "short" arcs, depending on whether the interelectrode gap is large or small. The value of the arc rotation rate, ω (which ranges between approximately 50 and 1000 sec^{-1}) had a considerable bearing on the thermal efficiency of short-gap arcs because of the dependence of the convective losses on it. Since the chamber gases radiated much more strongly than air uncontaminated by electrode material, convective and radiative losses are distinguished by solving for first-power and fourth-power dependence on temperature difference with the walls; the convective losses are examined in conjunction with a vortex model of the gas behavior.

The Johns Hopkins University
APPLIED PHYSICS LABORATORY
Silver Spring, Maryland

TABLE OF CONTENTS

The Johns Hopkins University
APPLIED PHYSICS LABORATORY
Silver Spring, Maryland

LIST OF ILLUSTRATIONS

The Johns Hopkins University
APPLIED PHYSICS LABORATORY
Silver Spring, Maryland

1. INTRODUCTION

This paper is concerned with the heat losses occurring in high-power (~15 Megawatt input), electrothermal (plasma arc) heaters which operate at bulk enthalpies up to 2500 Btu/lb. The production of dense plasmas is of considerable importance in the simulation of high velocity flight; three such heaters are presently in use at The Johns Hopkins University Applied Physics Laboratory to supply air at temperatures up to about 7000°R for such purposes as the operation of full-temperature simulation hypersonic tunnels, supersonic combustion ducts, and tunnels for testing re-entry ablation materials (Ref. 1). These heaters make use of a split-electrode system that generates a self-induced magnetic field for the purpose of rapidly moving the arc around the electrodes, thereby eliminating the need for an external field coil. This approach was dictated by the characteristics of the available power supply, a large submarine battery (Ref. 1), that favor the use of large currents but not of high voltages.

Of the three main heat loss mechanisms, arc radiation, gas radiation, and convection, the last two were believed to be predominant because of the wide variation of overall efficiency, depending on the choice of operating variables. Any continuously rotating arc generates a strong vortex, and the efficiency was found to be a function of the arc rotation rate (which varied between 50 and 1000 sec^{-1}, depending mainly on current and pressure). It was important to know the relative proportions of forced convection and radiation losses at moderate enthalpies to provide

a rational basis for reducing convective losses to a minimum and to obtain information on gas emissivities that would be useful in indicating what limit would be placed on chamber size when much higher enthalpy running was undertaken, since it was suspected that calculations based on pure air radiation tables would be inapplicable.

In this paper, the electrode operation is first described. The relationship between arc rotation and current, pressure, and electrode gap is then investigated for a split-ring arc. The measurement of arc rotational velocity having been dealt with, the effects of the vortex and the chamber geometry on heat transfer are then discussed, and a model is advanced to account for the observed effects.

2. NOTATION (Excluding Constants)

a	Distance between center lines of electrodes, ft
A	Area, ft^2
b	Width of arc chamber, ft
B	Field strength, lines cm^{-2}
C_d	Drag coefficient, dimensionless; discharge coefficient, dimensionless
c_p	Heat capacity at constant pressure, $Btu(°R)^{-1}\ slug^{-1}$
d	Diameter of arc chamber, ft; length parameter in Reynolds and Nusselt numbers, ft; diameter of arc column, cm
$f(\ell)$	Arc gap function (= 2 ln [(ℓ+R)]), dimensionless (see Eq. (1))
$f(\dot{q})_n$	Geometrical function (= x^c), Btu $ft^{1.6}\ sec^{-1}(°R)^{-1}$ (see Eqs. (5-9))
$f^c(T)$	Convective function (= $(T_g - T_w)(\omega/\nu)^{0.8}$, $(°R)\ ft^{-1.6}$
$f^r(T)$	Radiative function (= T_g^4), $(°R)^4$
h	Film coefficient, Btu $ft^{-2}\ sec^{-1}(°R)^{-1}$
H	Enthalpy, Btu lbm^{-1}
I	Discharge current, amps; radiation intensity per unit volume, Btu $ft^{-3}\ sec^{-1}$
k	Thermal conductivity, Btu $ft^{-1}\ sec^{-1}(°R)^{-1}$
L	Length, ft
ℓ	Interelectrode gap, ft (unless otherwise stated) Effective length of arc track, ft
$\dot{m}$	Mass flow, lbm sec^{-1}

Nu	Nusselt number (= hd/k), dimensionless
p	Electrode perimeter, ft
P	Pressure, psia (unless otherwise stated); heat power, Btu sec^{-1}
Pr	Prandtl number (= $c_p \mu/k$), dimensionless
$\dot{q}$	Heat flux, Btu $sec^{-1} p$
r	Radial distance, cm or ft
R	Gas constant (= 1716), $ft^2 sec^{-2} (°R)^{-1}$; cross-sectional radius of electrode, ft
Re	Reynolds number (= $dv\rho/\mu$), dimensionless
St	Stanton number $h/V\rho c_p \mu$), dimensionless
T	Temperature, °R
v	Discharge voltage, volts
V	Volume of arc chamber, ft^3; velocity, ft sec^{-1}
x_n^c	Geometrical function (= $f(\dot{q})_n$), Btu $ft^{1.6} sec^{-1} (°R)^{-1}$
x_n^r	Geometrical function (= $2\sigma V(\epsilon/L)A_n/A_{total}$), Btu sec^{-1} $(°R)^{-4}$
Z	Compressibility factor, dimensionless
γ	Ratio of specific heats, dimensionless
ϵ/L	Emissivity per unit thickness, ft^{-1}
η	Overall efficiency (fractional)
μ	Dynamic viscosity, slug $ft^{-1} sec^{-1}$
ν	Kinematic viscosity, $ft^2 sec^{-1}$
ρ	Mass density, slug/ft^3
σ	Boltzmann's constant (= 4.81×10^{-13}), Btu $ft^{-2} sec^{-1}$ $(°R)^{-4}$
ω	Arc rotation rate, sec^{-1}

Subscripts

c	Convective
cyl	Cylindrical section
elec	Electrode
end	End plate
forced	Forced vortex
g	Gas
h	Hydraulic
i	Cooling channel designation
induced	Induced vortex
m	Metering; run designation
n	Surface exposed to heating
p	Constant pressure
r	Radiative
t	Stagnation
w	Wall
o	Standard electrode gap (= 0.141 ft)
1	Radius of arc chamber exit duct
2	Radius of equivalent circular arc path
3	Outer radius of arc chamber

Superscripts

*	Sonic value
'	Unheated condition

A bar ($\bar{}$) indicates a mean value

3. EXPERIMENTAL APPARATUS AND MEASUREMENTS

3.1 Arc Operation and Overall Design--The design of an arc unit has much in common with that of a magnetohydrodynamic duct. The essence of the design used here is the use of the rail accelerator (Refs. 2-4) electrode system, which has been adapted for continuous DC operation by making it re-entrant; this principle has now been in use for some years in arc heaters in various laboratories, both with three-phase AC (Refs. 5-7) (three or four electrode types) and with DC (Refs. 8-13) (two electrode types) power supplies. Operational experience in the latter mode--which is the more satisfactory of the two--has been gained over the range of current values $8 < I < 32$ kamps. Figure 1 shows a cut-away view of the unit, the details of many of the components of which are similar to those of a steel arc described in Ref. 9. The pressure vessel or heat exchanger, in which the arc rotated, was made of forged chrome copper to combine sufficient strength with high thermal conductivity for cooling purposes; it consisted basically of a cylindrical section of internal diameter 19.75 inches closed by two end plates spaced 11 inches apart. These three sections were in electrical contact, but the unit as a whole was electrically floating since the power supply to the electrodes was grounded during discharge. Cooling channels were also machined within all the main components of the pressure vessel. Since welding of such large copper masses was not feasible, copper tapered plugs were driven into all holes that required closing.

The air flow system was a "hard" one, i.e., the pressure chamber was located between two sonic orifices. The first orifice was used for flow

THE JOHNS HOPKINS UNIVERSITY
APPLIED PHYSICS LABORATORY
SILVER SPRING MARYLAND

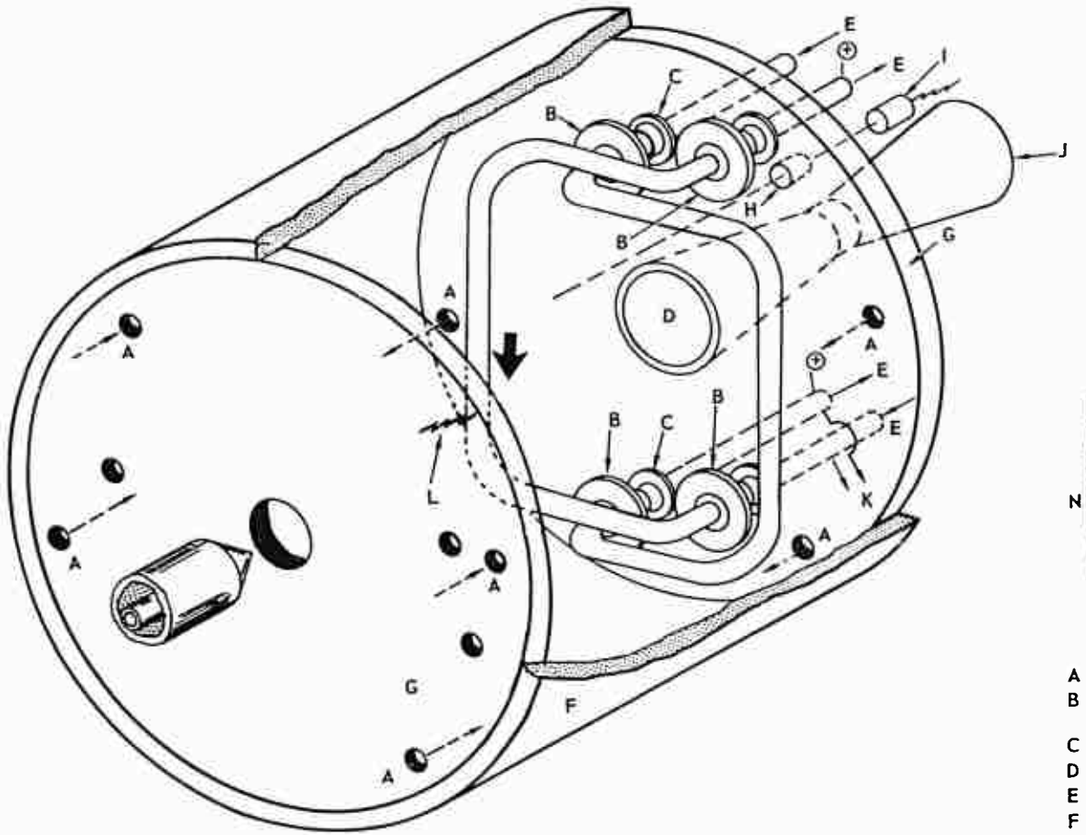

COOLING CIRCUITS ARE INCORPORATED IN THE CYLINDRICAL END PLATES G

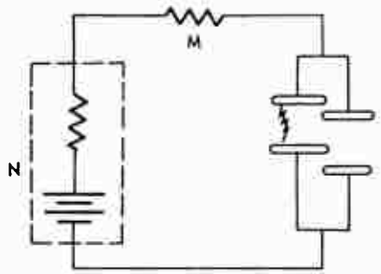

LEGEND

- A AIR ENTRY PORTS
- B INSULATOR RADIATION SHIELDS (INTEGRAL WITH ELECTRODE POSTS)
- C INSULATOR COVERS
- D DISCHARGE ORIFICE
- E COOLANT FLOWS
- F CYLINDRICAL SECTION
- G END PLATE
- H ROTATION PICKUPS
- I PHOTOCELL
- J EXIT NOZZLE
- K ROTATION PICKUPS
- L ROTATING ARC COLUMN
- M BALLAST RESISTANCE
- N BATTERY POWER SUPPLY

Fig. 1 DIAGRAMMATIC CUTAWAY VIEW OF ARC AIR HEATER

metering, and the second, the discharge orifice (which served when required as the throat of a supersonic nozzle), was also used for enthalpy measurement, provided that the double condition for choking flow

$$(1/0.548)P_{\text{ambient, cold}} < P_{\text{chamber, hot}} < 0.528P_{\text{upstream, cold}}$$

could be satisfied during running.* Process air entered the unit mainly through eight holes distributed around the periphery of the chamber; a proportion of the air was also allowed to enter through the insulators to promote a plasma-free region around the points where the electrode stems passed out of the chamber. If the whole air flow had been introduced inside the annular arc path, it would then have been free to make a short cut to the discharge orifice without participating effectively in the heating process.

The various cooling channels were provided with inlet and outlet thermocouples and flow meters of the drag disk type. The outputs of these (together with that of an entry-air thermocouple) were scanned every 2.25 sec by a digital data acquisition system and the results recorded on magnetic tape for subsequent reduction in the form of a progressive heat balance.

---

* The factors 0.528 or $0.548\left[= \left(\frac{\gamma+1}{2}\right)^{-\gamma/(\gamma-1)}\right]$, appropriate to either "cold" or "hot" air, may be as high as 0.8 if a diffuser is fitted to extend the sonic orifice (Ref. 15).

3.2 Electrode Design--For a short, easily variable electrode gap,* a facing configuration is convenient in the absence of the need for an external magnetic field. Experience has clearly demonstrated the advantages of such electrodes being constructed of straight lengths of tubing; the actual form used being that of a square with rounded corners. This preserved the required ring character while eliminating the radial magnetic field necessary to counteract the radial component of induced magnetic field that causes the "bowing out" of an arc observed with electrodes having purely radial symmetry. The electrode system, which was cooled by high velocity water (Ref. 14), comprised two pairs of interleaving hollow copper arms, each pair projecting from one of the end plates; the gap between the pairs of arms was normally set at 1-1/4 inch, but larger or smaller values could be used, depending on the discharge voltage required. Each end plate thus supported four electrode posts. These posts were mounted in lucite insulators protected by covers made of fused silica or nonhygroscopic boron nitride; these covers were, in turn, shielded from direct arc radiation by "skirts" formed integrally with the electrode posts. No problem arose as a result of cooling connections forming numerous high-impedance, parallel leakage paths to ground.

3.3 Arc Rotation Measurement--Two different devices were used:

1. In the Original arrangement (Ref. 16), a photocell looked obliquely (i.e., slightly off-axis) through the chamber exit orifice towards a point on or near the annulus swept by the arc, and thus picked up light level changes as the arc rotated. For the present

*As a matter of terminology, the word "gap" is used here to describe the distance between positive and negative electrodes, while "split" refers to the much shorter distance between the parallel overlapped arms of the same electrode.

type of chamber, this arrangement was preserved in principle, but the photocell was arranged to look through a window (Ref. 9) in the wall of the arc chamber in a direction tangential to (and at right angles to) both electrodes (Fig. 1).*

2. The inductive pulse developed as the arc jumped an electrode split was later isolated and suitably filtered to pass only a signal in the frequency range of arc rotation (Fig. 2(a)). In an improved form of the circuit (Fig. 2(b)) a neon lamp/photocell pickup was substituted for the isolation transformer. The electrodes thus acted as their own search coil. Figure 2 (c) shows a typical output trace generated by the latter form of circuit.†

3.4 Stagnation Temperature/Enthalpy Measurement--Three methods of stagnation air temperature measurement were employed:

1. Heat Balance. A computer program was used to determine the summation of losses from the water flows and their respective temperature rises. If the flows in the various channels are w_1, w_2, ... and the respective temperature rises are ΔT_1, ΔT_2, ... , the program determined $|w\Delta T|$, where

$$w\Delta T = [w_1,\ w_2 \ldots w_i] \begin{bmatrix} \Delta T_1 \\ \Delta T_2 \\ \cdot \\ \cdot \\ \cdot \\ \Delta T_i \end{bmatrix} .$$

*A similar arrangement has since been used elsewhere (see, e.g., Ref. 17).

†The author acknowledges the assistance of his colleagues R. T. Cusick and M. E. Rose in the development of these circuits.

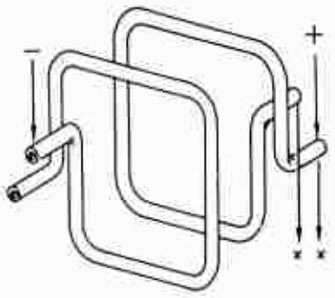

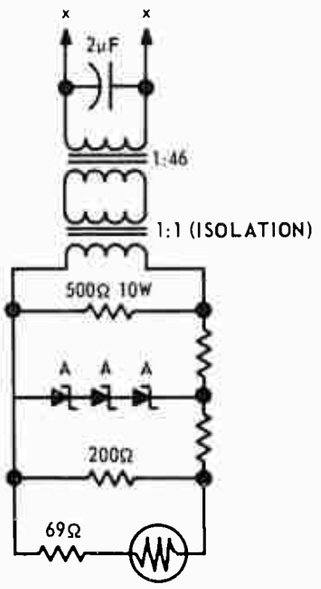

C.E.C. OSCILLOGRAPH
(0.533 V/in., 1000 c.p.s. GALVO RESPONSE)
A ZENER DIODES IN 1605 12V, 10W

(a) ORIGINAL CIRCUIT

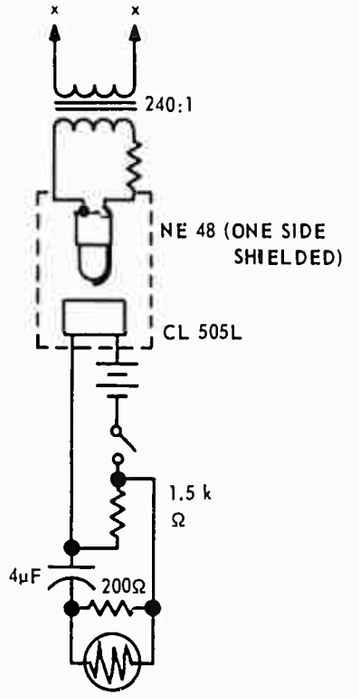

C.E.C. OSCILLOGRAPH
(0.533 V/in., 1000 c.p.s. GALVO RESPONSE)

(b) IMPROVED CIRCUIT

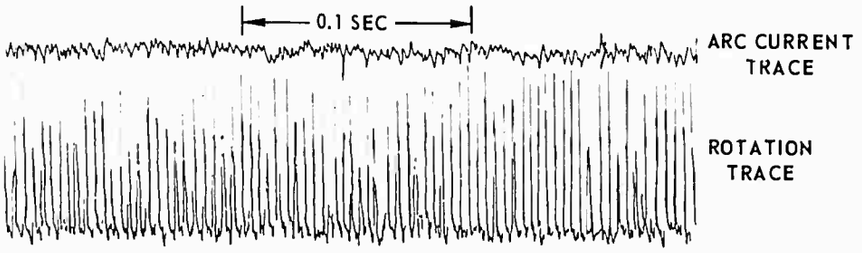

(c) TYPICAL ROTATION TRACE (ω = 255 SEC $^{-1}$)

Fig. 2 INDUCTIVE ROTATION MONITORING CIRCUIT

Values of $w_1\Delta T_1$, ... $w_i\Delta T_i$ were printed out. This computation was performed every scan, several scans being necessary for thermal equilibrium to be established. The overall efficiency was then given by

$$\eta = 1 - \frac{c_p\, w\Delta T}{\overline{VI}} ,$$

where analogue data were used to obtain the mean input power $\overline{VI}$ from separate voltage and current records. The total (bulk) enthalpy was determined from

$$H_t = H' + \frac{\overline{VI}\,\eta}{\dot{m}} ,$$

where H' is the enthalpy of the incoming air. Appropriate charts were then used to convert from enthalpy to temperature (Ref. 18).

2. Pressure Measurement. (a) For one-dimensional sonic flow from the arc chamber, total enthalpy may be determined from the arc chamber parameters by means of the expression (Refs. 18 and 19)

$$\frac{\dot{m}}{P_t A^*_{ex} C_{d_{ex}}} = \frac{280}{H_t^{0.387}} \text{ lbm sec}^{-1}\text{atm}^{-1}\text{ft}^{-2} ,$$

which is almost independent of pressure level. Unfortunately, $C_{d_{ex}}$ is difficult to determine accurately under "hot" conditions; it is associated with a value of Re based on throat diameter reduced about ten-fold over the cold value, but the actual increase of $C_{d_{ex}}$ over the cold value is slight (about 2%). (b) Winovich

(Ref. 19) has shown how the enthalpy of the hot condition may be evaluated from the expression

$$\frac{(P_t)_{hot}}{(P_t)_{cold}} = \frac{[\dot{m}/A^*_{ex}\, P_t\, C_{d_{ex}}]_{cold}}{[\dot{m}/A^*_{ex}\, P_t\, C_{d_{ex}}]_{hot}}$$

$$= \frac{\text{constant}}{[\dot{m}/A^*_{ex}\, P_t]_{hot}} \cdot \frac{C_{d_{ex,\ adiabatic}}}{C_{d_{ex,\ diabatic}}} .$$

A heat transfer effect and boundary-layer correction can be taken into account to afford an estimate for the ratio of adiabatic to diabatic C_d's. This approach was used to obtain the best comparison with heat balance results for runs using different exit orifices, even though the orifice geometry differed somewhat from that assumed for the boundary-layer calculation. It is obvious that very strong values of swirl can so alter C_d (Ref. 20) as to vitiate this approach.

3. Pyrometer and Ablating Probe. For certain tests an ablating probe of a material such as graphite was inserted in the jet and observed with a miniature photovoltaic pyrometer (Ref. 21). Such observations gave a lower limit to the stagnation temperature of the jet; the subliming temperature of the material however imposed an upper limit on the measurement that could be obtained.

4. PONDEROMOTIVE FORCE AND AERODYNAMIC DRAG

Radial magnetic field effects associated with the four, 90° electrode corners are here disregarded. The electrodes were considered to be infinitely long straight conductors carrying current. Considering the electrode system shown in Fig. 3, the field at distance r from one conductor due to current flowing through the electrode up to the arc is, for $B_z = H_z$ in air,

$$B_z = \frac{1}{2} \frac{2I_y}{10r} \text{ lines cm}^{-2},$$

where I_y is in amperes and r is in cm. On an element, dr, of an arc carrying a current I_x, the force is

$$\frac{B_z I_x \, dr}{10} \text{ dynes}.$$

[Note that $B_z I_x$ is the only significant term in the vector

$$\vec{B} \times \vec{I} = \vec{i}(I_y B_z - I_z B_y) + \vec{j}(I_z B_x - I_x B_z) + \vec{k}(I_x B_y - I_y B_x).]$$

Over the whole length, ℓ, of the arc path the force is

$$\frac{I^2}{100} \int_R^{a-R} \left(\frac{1}{r} + \frac{1}{a-r}\right) dr = \frac{I^2}{100} \left[\ln \left(\frac{a-R}{R}\right)^2\right] = \frac{I^2}{100} \left[\ln \left(\frac{\ell+R}{R}\right)^2\right] \text{ dynes}.$$

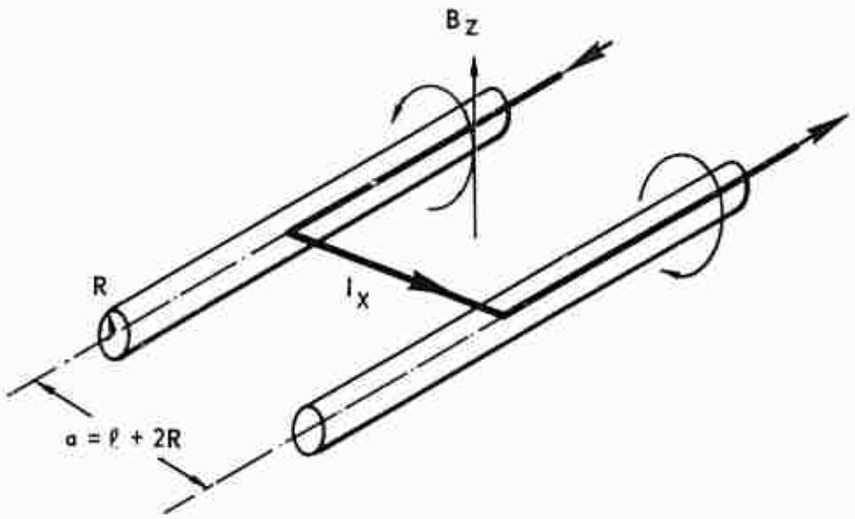

Fig. 3 CURRENT FLOW BETWEEN PARALLEL RECTILINEAR ELECTRODES

Considering an arc as a cylinder of diameter, d, and length, ℓ, opposed by an aerodynamic drag force,

$$\frac{I^2}{100}\left[2\ln\left(\frac{\ell+R}{R}\right)\right] = \tfrac{1}{2} C_d \rho \ell d V^2 ;$$

hence,

$$V = \frac{I\sqrt{2}}{10\sqrt{C_d \rho \ell d / f(\ell)}} , \qquad (1)$$

where $f(\ell) = 2\ln[(\ell+R)/R]$.

Substituting $\rho = P/RTZ$ in Eq. (1),

$$V = \frac{I}{10}\sqrt{\frac{2Tf(\ell)\,RZ}{P \ell d C_d}} = \omega \mathcal{L} , \qquad (2)$$

where $\mathcal{L}$ is the arc perimeter track and ω the number of arc rotations per second.

The determination of the appropriate value of the length $\mathcal{L}$ of the arc track was made on the basis of the plan views shown in Fig. 4, which indicate the basic values chosen for the two extreme forms of electrode used. Observation of electrode discoloration and of films of arc behavior indicated that, for example, the curved parts of the posts (out of the main electrode plane) also shared to some extent in conveying current, but it was difficult to make adequate allowance for this. The velocity, V, is a low subsonic value as far as hot gas is concerned, so that $T \approx T_t$ and $P \approx P_t$. To make the ratio $f(\ell)/\ell$ equal to unity at the standard value of gap, one may write

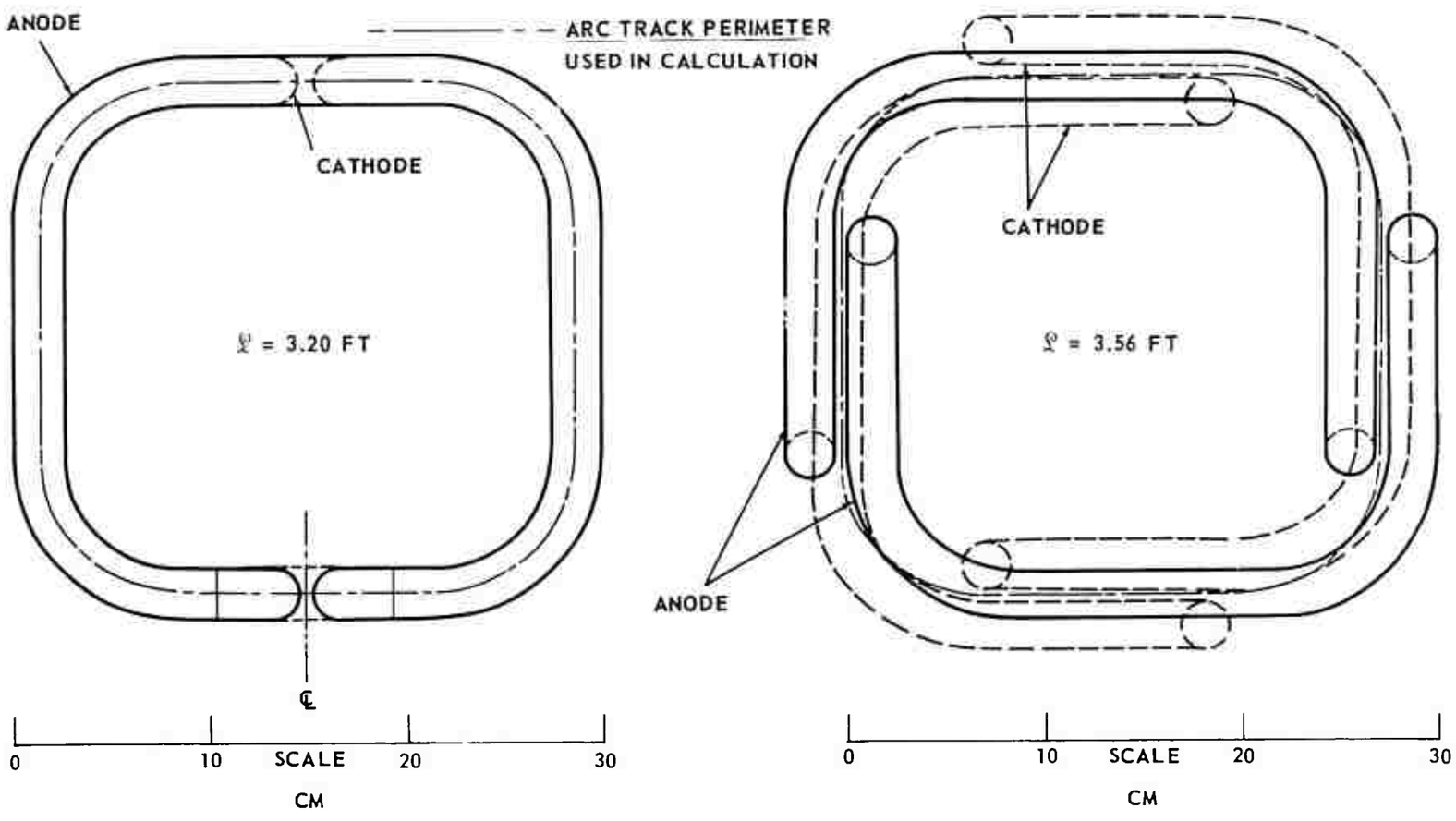

(a) PLAN OF BUTT-TYPE ELECTRODES

(b) PLAN OF DOUBLE-OVERLAP ELECTRODES

Fig. 4 CALCULATION OF ARC TRACKS

$$\frac{\omega \mathcal{L}}{L\sqrt{T_t}} \sqrt{\frac{\ell f(\ell_o)}{\ell_o f(\ell)}} = C\, P_t^{-\frac{1}{2}} , \qquad (3)$$

$$\text{where } C = \frac{1}{10}\sqrt{\frac{2RZ\, f(\ell_o)}{C_d\, d\, \ell_o}} .$$

Points representing the value of the first term in Eq. (3) are plotted in Fig. 5. Scatter is ascribed partly to lack of precision in calculating $\mathcal{L}$ and partly to the fact that average rotation rates have been used. Where the rotation rate was steady, the value is not in question, but occasional "hold-ups" reduced an otherwise steady rate. The line of best fit, drawn at a slope of $-\frac{1}{2}$, is used to obtain an experimental value of C. The bifurcation occurring with overlapped electrodes is also believed to contribute to a small lowering of the rotational velocity, following a current reduction in the separate limbs of an overlap.

For an open air arc, Eq. (2) cannot be further reduced, but, for a choking arc, $P_t = P_t(\dot{m}, T_t)$. Further manipulation did not appear to be justified, however, as the parameters controlling rotation were considered to be established.

It is of interest to determine the value of d from the above expression. Assuming $C_d = 2$ (flat plate), a typical value of d was 4.86 cm. From observation of the luminous column (Fig. 6(b)), $d \approx 5$ cm.

4.1 Rotation Breakdown at Extended Gap--Since the field is much weaker midway between the split-ring electrodes, operating at relatively wide gap, than at the edges of the electrodes, the concept of the arc as a solid body will lead to an imbalance of driving field and opposing force in the central portion of such a gap. The validity of

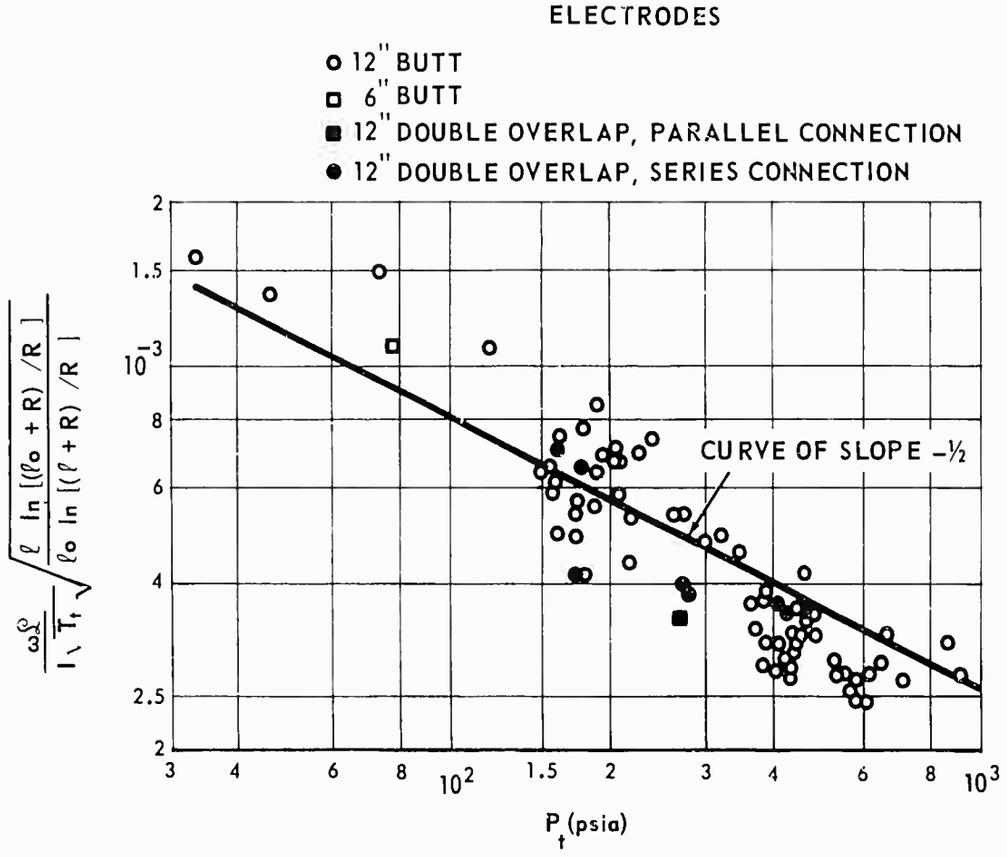

Fig. 5 ROTATION RATE CORRELATION

the expression for arcs of different horizontal lengths was therefore investigated experimentally. The arc shown in Fig. 6(a) (ℓ = 3 inches) was being dragged along by its roots (the actual arc image is blurred because of the length of exposure of one frame of the film), but when the gap was extended beyond about 6 inches, the rotational behavior became irregular. Figure 6(b) illustrates a "long" (ℓ = 18 inches) gap where the rotation in the central region has collapsed. In such a case, the precise mode of attachment of the arc to the electrodes was not clear; it appeared quasi-diffuse, with vestigial rotation. The impression was given that the form the electrode structure could take was arbitrary since arc filaments were seen to attach at almost any conducting point. (From other evidence, however, it is not believed that the electrode form is arbitrary.) It is probable that such unrotated arcs as those of Eschenbach, et al. (Ref. 22) are of this long type.

In view of the change of character of the arc as the gap was raised, measurements of voltage versus gap were made at atmospheric pressure, using the apparatus shown in Fig. 6(b). It was deduced that there was no significant voltage change as the arc character changed from short to long, the consistent relationship being

$$v \propto \ell^{0.45}$$

nor was any significant difference in the gap/voltage relationship between butt and overlapped types of electrodes observed.

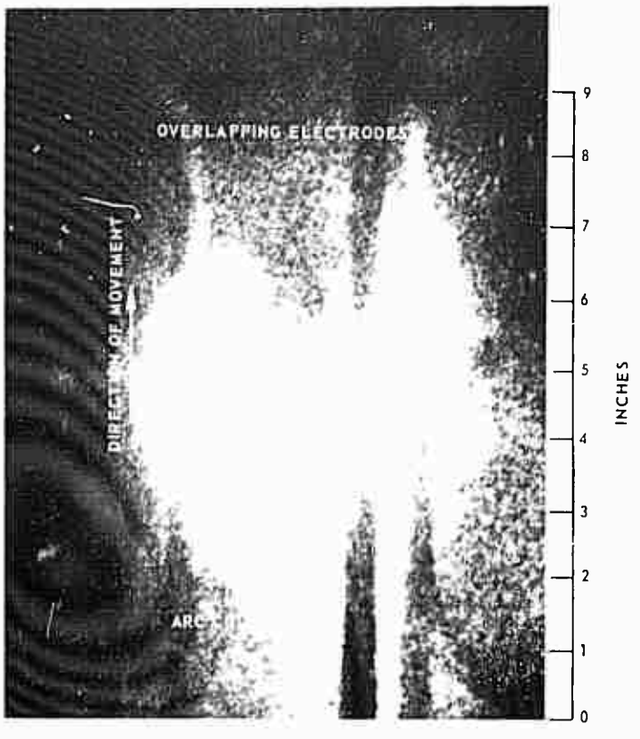

(a) SHORT GAP

(PRINTED THROUGH RED FILTER)

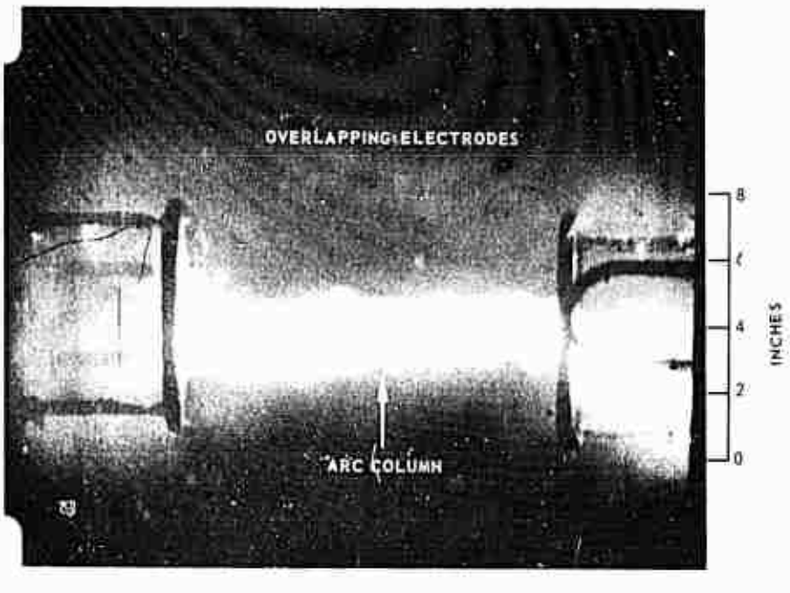

(b) LONG GAP

(PRINTED THROUGH DOUBLE YELLOW FILTER)

Fig. 6 TYPICAL APPEARANCE OF ARC COLUMN

5. ANALYSIS OF HEAT LOSSES

In general, three major sources of loss of input energy occurred: (a) radiation from the arc itself; (b) radiation from the volume of gas in the chamber; and (c) forced convective heat transfer from the gas swirl set up by arc rotation. These energy losses were all absorbed by the cooling water. In one set of experiments (Ref. 23) where radiant energy calculations for a high pressure (rotating) arc were quoted, losses other than radiation were neglected so that the energy balance was given by

$$\dot{m}\,\Delta H = P - IV\ ,$$

where ΔH = enthalpy addition,

I = intensity of radiation per unit volume (radiated into 4π steradians),

V = chamber volume, and

P = heat power input.

However, although the claim was made that the experimental results fell amazingly close to theory, it was clear from an examination of the plotted points that the temperatures were so low that the corresponding "radiation-loss" lines had not, or had hardly, diverged from the "no-radiation-loss" line. Since then $IV \approx 0$, nothing was proved regarding coincidence of experimental results and theory, which was unfortunate since any experimental evidence of a contamination effect was of considerable interest. It was felt that this particular basic assumption

offered no guidance, and it was therefore necessary to approach the problem by a different route.

5.1 Arc Radiation --The individual heat loss by radiation from an arc is difficult to estimate. From observation of the thermal attack on the cylindrical section of an earlier steel arc case, and from the general ablation pattern on boron nitride liners on smaller arc units, the main effect was seen across a band about 2 inches wide on the cylindrical section immediately outside the path of the arc. The proportion of heat lost in this way was believed to be small in proportion to the rest, except possibly in the case of the electrodes. An assessment of the importance of the direct radiation in the total heating was made indirectly by the following experiment.

In an attempt to improve efficiency by absorbing as much as possible of the radiation emitted by the arc itself, the effect of injection of a relatively small quantity of absorbent (< 10% of air flow by weight) was investigated. A powder feeder originally designed for handling alumina was adapted for use with graphite (which acts as its own lubricant). The results of runs of long duration are shown in Fig. 7; the running conditions are given in Table I. The figure shows that the heat loading on the case was increased while the gas enthalpy was decreased by graphite injection,

Table I

Arc Conditions for Graphite Injection Runs

Run	Air Flow Rate, pps	Powder Flow Rate, pps	P_t, psia	Input Power, MW	
				Powder Off	Powder On
271	0.41	0.025	23	2.04	1.92
272	0.41	0.017	23	2.04	1.87
273	0.41	0.012	23	2.04	1.89
274	0.41	0.033	23	2.03	1.87

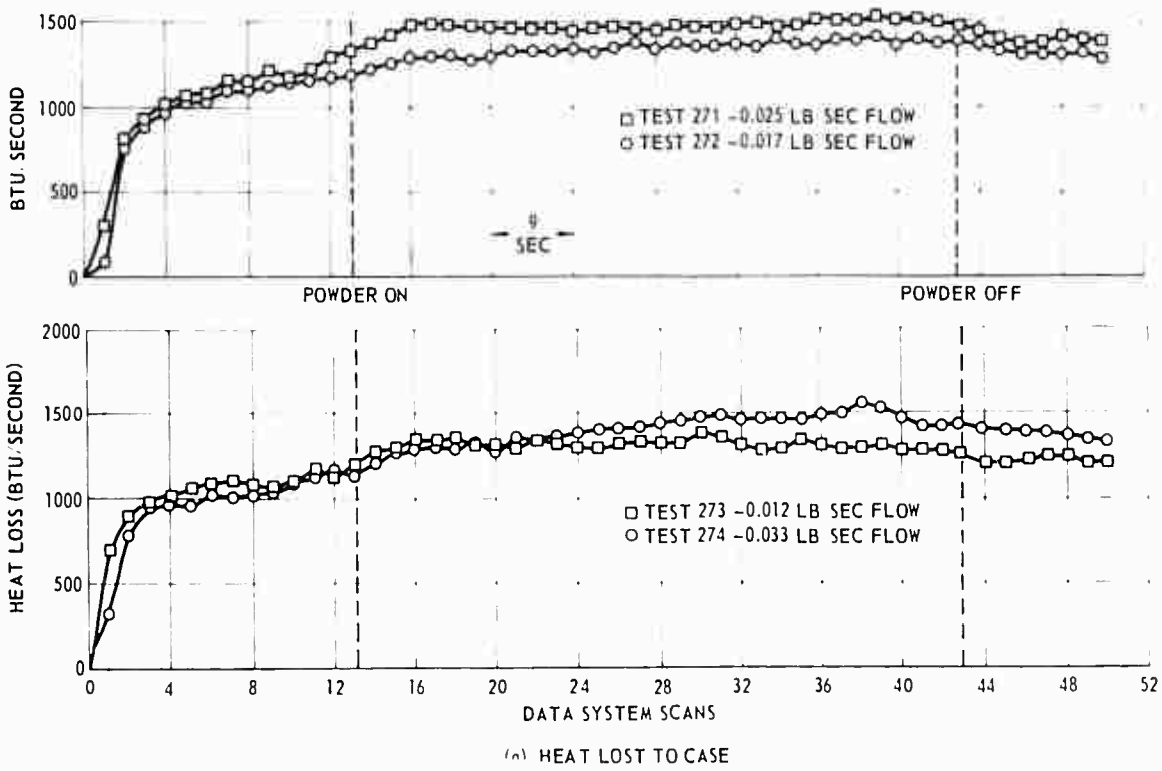

(a) HEAT LOST TO CASE

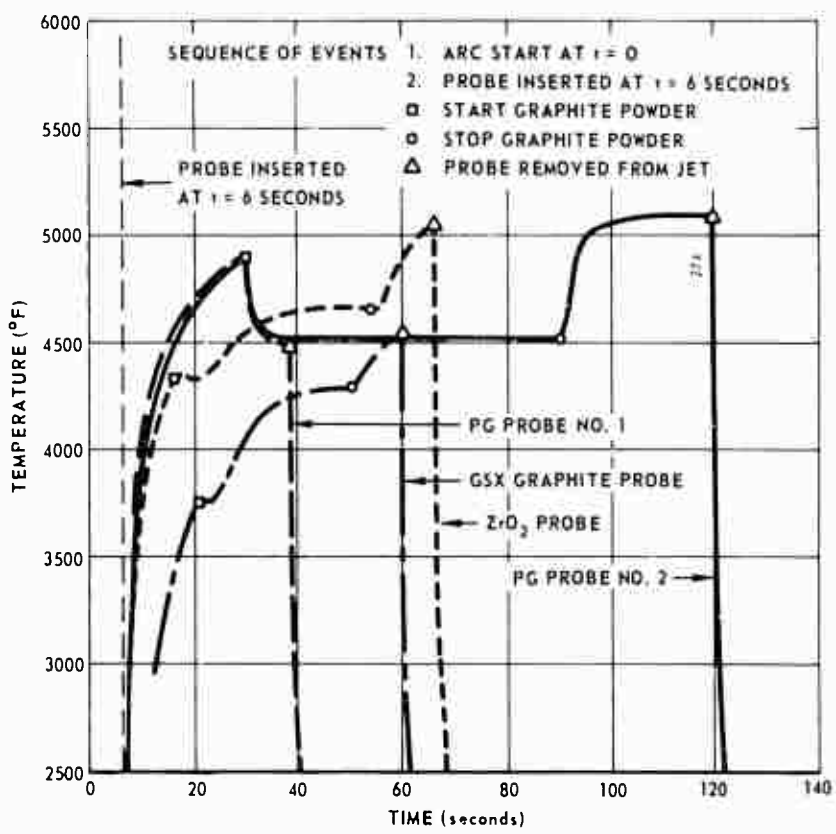

(b) TEMPERATURE OF PROBES

Fig. 7 CONDITIONS DURING GRAPHITE INJECTION

the latter effect being checked by means of the pyrometer-and-ablating-probe method of temperature measurement, using graphite and zirconia samples.* This result indicated that the general gas radiation was increased by graphite injection (probably due to the carbon monoxide bands). Observation of the emerging jet showed an increase in luminosity in the red region. From the high opacity of the (cold) carrier gas, and the fact that a large amount of graphite passed through the arc without being burned up, it was concluded that, though the graphite was probably an effective absorber of arc radiation, the effect of the arc radiation was small compared to that of the radiation emanating from the gas itself. This conclusion was strengthened by the fact that the overall efficiency of an arc unit could be caused to vary between about 5 and 50% by suitable choice of running conditions (see below) even though the power input varied little. To test this hypothesis arc radiation was therefore neglected in the analysis to follow.

5.2 Forced Convection--It had previously been suggested that the swirl imparted to the gas by an arc affected the heat transfer (Ref. 7). This was specifically demonstrated by short-circuiting part of the ballast resistance during certain runs† so that the current (and therefore the rotation rate) was caused to increase by a relatively large amount (about 25%). The chamber pressure remained almost constant throughout the runs, showing that a decrease in efficiency almost

---

*Acknowledgment is made to Messrs. M. L. Hill and J. M. Akridge for their assistance in this part of the program and to Dr. W. H. Avery for his original suggestion regarding this approach.

†The runs designated 5 and 6 in Table II represent the earlier and later conditions of such a run.

compensated for the increase in input power ($\propto$ current, since the voltage did not change under these circumstances). Corresponding effects were produced in a unit in which an external field could be varied to change the rotation rate at constant current. When the overall efficiency was plotted against the rotation rate, a strong connection emerged, which transcended the individual effects of pressure and current (Fig. 8).

Consider now the simple vortex flow model shown in Fig. 9. Let r_2 be the radius of the circle whose circumference is equal to the arc track, computed as indicated above, and let r_3 and r_1 be the radius of the cylindrical chamber wall and that of the exit duct, respectively. The induced vortex rV = constant ($r_2 < r < r_3$) gives

$$V = 2\pi r_2^2 \omega / r ,$$

and therefore,

$$V_3 = \pi \frac{d_2^2}{d_3} \omega .$$

The air velocity V_2 is here assumed to be equal to $\omega \mathcal{L}$, where ω is now considered to be a uniform angular velocity. For example, for $\omega = 100$ sec^{-1} and $d_2 = 1.13$ ft, $V_3 = 207$ ft sec^{-1}. For the forced vortex ($r_1 < r < r_2$),

$$V = 2\pi r \omega .$$

The variation of velocity in the respective vortices is sketched in relation to the superimposed axes in Fig. 10.

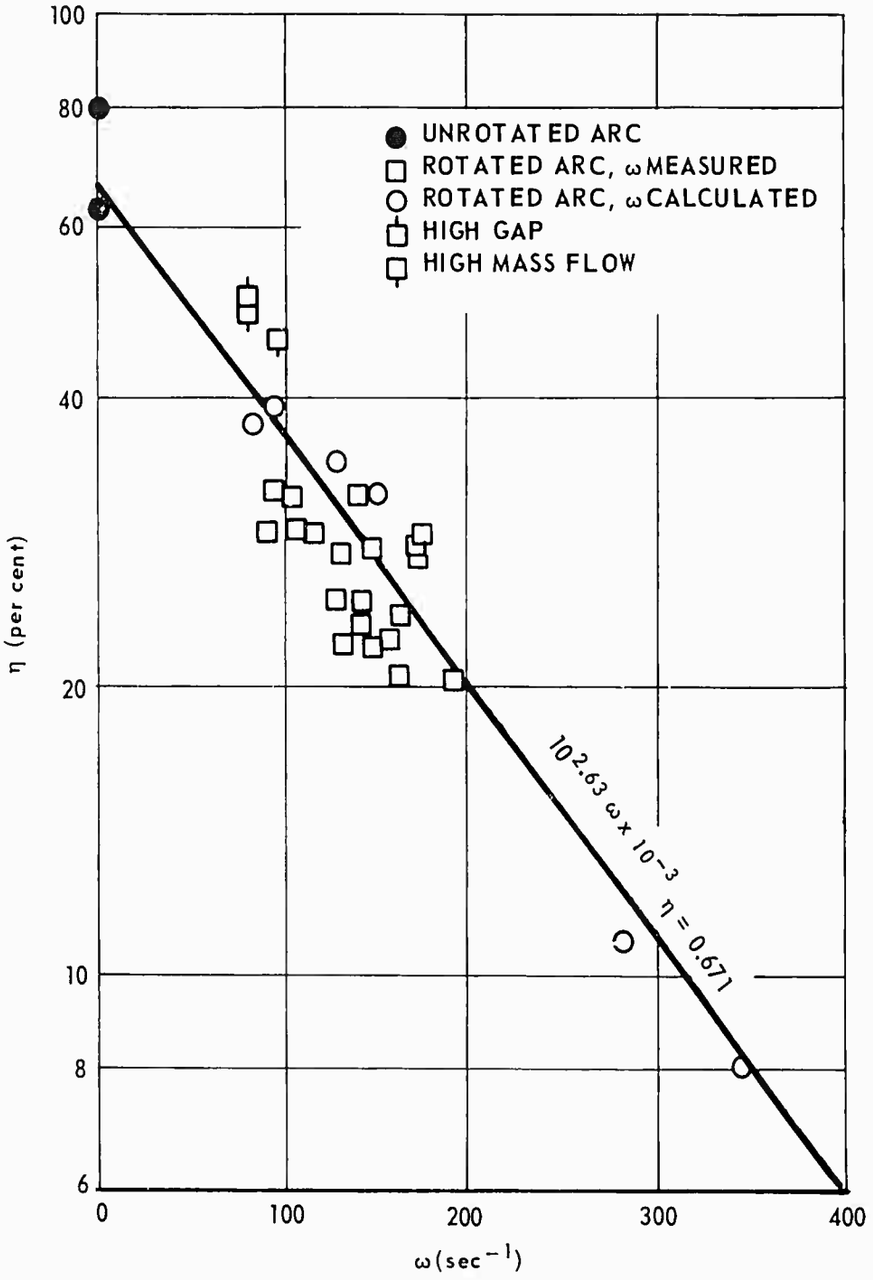

Fig. 8 ROTATION RATE VS OVERALL EFFICIENCY

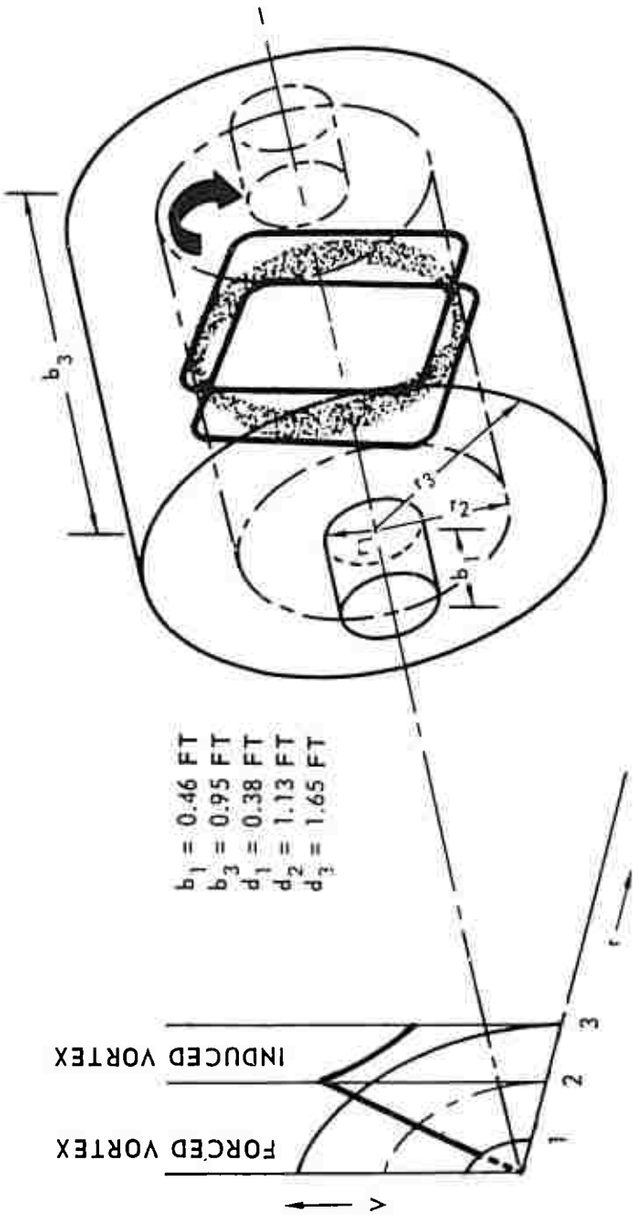

Fig. 9 MODEL OF VORTEX FLOW IN ARC CHAMBER

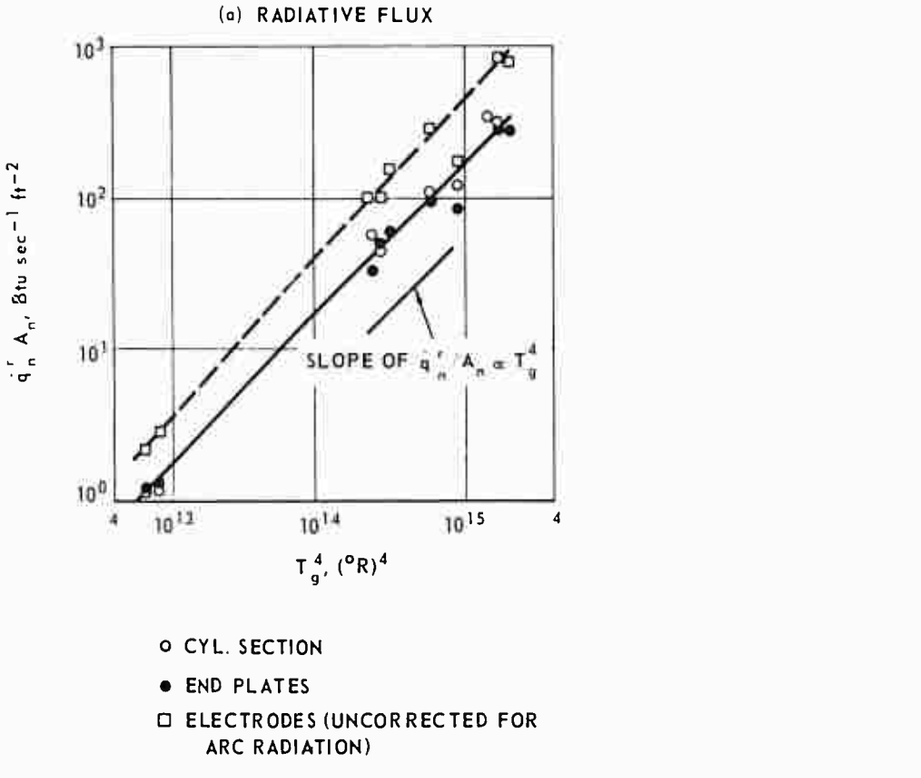

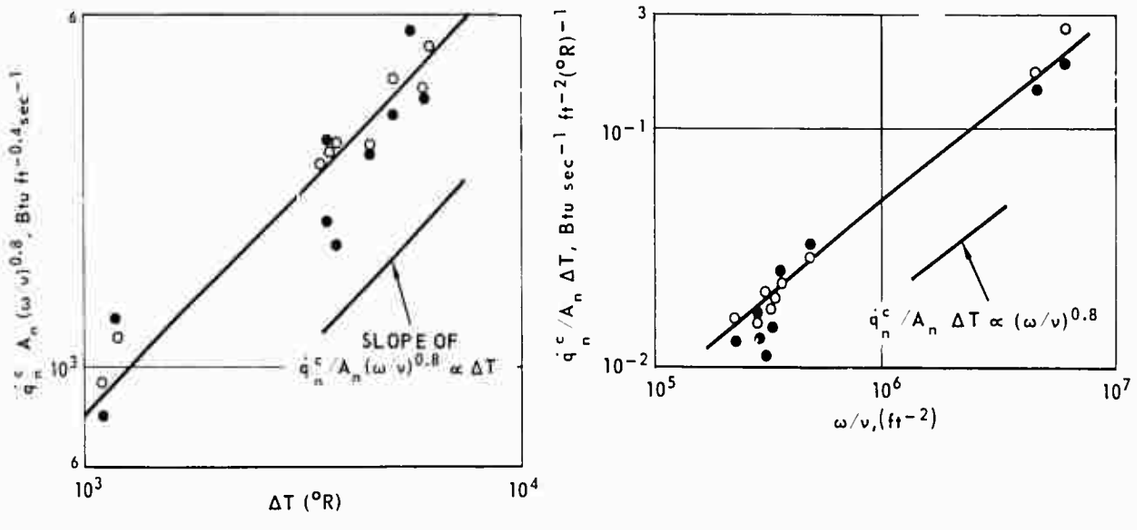

(b) FORCED CONVECTIVE FLUX

Fig. 10 CERTAIN SOLUTIONS FOR PROPORTION OF RADIATIVE AND CONVECTIVE FLUX

The heat flux to the walls may be simply expressed in terms of enthalpy and Stanton number as

$$A\dot{q} = St\,\dot{m}\,\Delta H ,$$

but in the case under consideration, the value of $\dot{m}$ is not defined. Instead, therefore, recourse was had to the Dittus and Boelter form of correlation:

$$Nu = C\,(Re)^{0.8}\,(Pr)^{0.33} , \qquad (4)$$

where the constant normally has the value 0.023. The characteristic length in the Reynolds and Nusselt numbers was defined by $4r_h$, where r_h is the hydraulic radius, as follows:

1. Cylindrical Section or Exit Duct.

$$r_h = \frac{\text{volume of chamber}}{\text{heat transfer area}} = \frac{\pi\, d_3^{\,2} b_3}{4\pi d_3 b_3} = \frac{d_3}{4} \text{ or } \frac{\pi d_1^{\,2} b_1}{4\pi\, d_1 b_1} = \frac{d_1}{4} .$$

$$\therefore \quad 4r_h = d_3 = 19.75 \text{ inches or } d_1 = 4.50 \text{ inches.}$$

The volume occupied by the electrodes was neglected as being small compared with that of the chamber (< 2% error).

2. End Plate.

$$r_h = \frac{\text{volume of annulus}}{\text{heat transfer area}} = \frac{2\pi\ r\ b_3\ \Delta r}{2(2\pi\ r\ \Delta r)} = \frac{b_3}{2} .$$

$\therefore\ 4r_h = 2\ b_3 = 22.88$ inches.

3. Electrode.

$$r_h = \frac{\text{cross-sectional area}}{\text{wetted perimeter}} = \frac{\pi R^2}{2\pi R} = \frac{R}{2} .$$

$\therefore\ 4r_h = 2R = 1$ inch.

The appropriate velocity may now be introduced into the Reynolds numbers for the various cases:

1. Cylindrical Section (induced vortex).

$$h = \frac{kC}{d_3} (Pr)^{0.33} \left(\frac{d_3 V_3}{\nu}\right)^{0.8} .$$

Dropping the stagnation subscript, since $T \approx T_t$,

$$\dot{q}^c_{\text{cyl, induced}} = Ah\Delta T = f(\dot{q})_{\text{cyl, induced}} (\omega/\nu)^{0.8} \Delta T = f(\dot{q})_{\text{cyl, induced}} f^c(T), \tag{5}$$

where $f(\dot{q})_{\text{cyl, induced}} = \pi\ b_3\ kC\ (Pr)^{0.33} (\pi\ d_2^2)^{0.8}$.

2. End Plate (induced vortex).

$$h = \frac{kC}{2b_3}(Pr)^{0.33}\left(\frac{2b_3V}{\nu}\right)^{0.8}.$$

$$\therefore \dot{q}^c_{end,\,induced} = \int_2^3 2\pi\, rh\,\Delta T\, dr$$

$$= f(\dot{q})_{end,\,induced}(\omega/\nu)^{0.8}\Delta T = f(\dot{q})_{end,\,induced} f^c(T), \qquad (6)$$

where $f(\dot{q})_{end,\,induced} = \frac{\pi kC}{1.2\, b_3^{0.2}}(Pr)^{0.33}(4\pi r_2^2)^{0.8}(r_3^{1.2} - r_2^{1.2})$.

3. End Plate (forced vortex).

$$h = \frac{kC}{2b_3}(Pr)^{0.33}\left(\frac{2b_3V}{\nu}\right)^{0.8}.$$

$$\therefore \dot{q}^c_{end,\,forced} = \int_1^2 2\pi\, rh\,\Delta T\, dr$$

$$= f(\dot{q})_{end,\,forced}(\omega/\nu)^{0.8}\Delta T = f(\dot{q})_{end,\,forced} f^c(T),$$

where $f(\dot{q})_{end,\,forced} = \frac{\pi kC}{2.8\, b_3^{0.2}}(Pr)^{0.33}(4\pi)^{0.8}(r_2^{2.8} - r_1^{2.8})$. (7)

4. Exit Duct (forced vortex).

$$h = \frac{kC}{d_1} (Pr)^{0.33} \left(\frac{d_1 V_1}{\nu}\right)^{0.8} .$$

$$\therefore \dot{q}^c_{cyl,\,forced} = f(\dot{q})_{cyl,\,forced} (\omega/\nu)^{0.8} \Delta T = f(\dot{q})_{cyl,\,forced} f^c(T) , \qquad (8)$$

where $f(\dot{q})_{cyl,\,forced} = \pi b_1 \, kC \, (Pr)^{0.33} \, (\pi d_1^{\,2})^{0.8}$.

5. Electrode (forced vortex).

$$h = \frac{kC}{2R} (Pr)^{0.33} \left(\frac{2R V_2}{\nu}\right)^{0.8} .$$

$$\therefore \dot{q}^c_{elec,\,forced} = A_{elec} h \Delta T = f(\dot{q})_{elec,\,forced} (\omega/\nu)^{0.8} \Delta T$$

$$= f(\dot{q})_{elec,\,forced} f^c(T), \qquad (9)$$

where $f(\dot{q})_{elec,\,forced} = \pi \, kC \, p \, (Pr)^{0.33} \, (2\pi R \, d_2)^{0.8}$.

The geometrical factors $f(\dot{q})_n$ for the various surfaces are constant for a given configuration, the main values being given in Table II.

5.3 Radiation from Chamber Gas--Calculated values of the radiation from normal, optically thin, air, given as the emissivity of a slab per unit thickness (ϵ/L), are available (Ref. 24).* For radiation from shapes other than plane, the total radiation per unit volume is defined as twice these values, since the "plane" then has two sides, namely $2\sigma(\epsilon/L)\,T^4$, where σ is Boltzmann's constant. Calculated values were suspected of being inapplicable; however, when values of $\dot{q}(\omega/\nu)^{0.8}$ were plotted, they were found to be roughly proportional to T^2, which suggested that gas radiation represented a larger fraction of the total radiation than would have been the case for pure air at the temperature of operation. It is known that contaminants could change gas emissivity by a factor of from 2 to 10 (Refs. 25 and 26).†

5.4 Separation of Radiative from Convective Losses--Neglecting direct arc radiation, then separating out quantities depending upon T and ω from the geometrical factors, we may write for the nth chamber surface of area A_n,

$$\dot{q}_n = x^r_n f^r(T) + x^c_n f^c(T)_n , \qquad (10)$$

where the unknown geometrical factors x^r_n and x^c_n are given by

$$x^r_n = \overline{2\sigma\ V(\epsilon/L)}\ A_n/A_{total},$$

and

---

*A higher actual emissivity than that given by Kivel and Bailey (Ref. 24) seems to be suggested by Ref. 26 (for higher temperature values).

†It is noted that the General Electric Company (Philadelphia) double-Gerdien type of arc employs very pure air, (Ref. 27) in order to minimize radiation losses and so permit operation at the highest possible enthalpy.

$$x^c_n = f(\dot{q})_n .$$

In addition, $f^r(T) = (T_g^4 - T_2^4)$, but since black body radiation from the wall can safely be neglected,

$$T_w^4 \ll T_g^4 , \text{ so}$$

$$f^r(T) = T_g^4 . \tag{11}$$

Also,

$$f^c(T)_n = (T_g - T_w)_n (\omega/\nu)^{0.8} . \tag{12}$$

Equation 10 may thus be written for all runs 1-m and surfaces 1-n for which a heat flux measurement is available:

$$\dot{q}_{1n} = x^r_n f^r(T_1) + x^c_n f^c(T_1)_n$$

$$\vdots$$

$$\dot{q}_{mn} = x^r_n f^r(T_m) + x^c_n f^c(T_m)_n$$

5.5 Results and Discussion--Apart from about 200 earlier runs conducted with steel arc components (not considered here on account of possible inconsistency arising from differing contamination products as the walls underwent ablation during running), 68 runs were made with only a copper cylindrical section, and of these, 24 runs were made with a complete copper shell; subsequently coated components

were used. From these 24 runs a few involving the best possible spread of temperature were selected for analysis. The electrode gap was, of course, sufficiently short in these runs (< 2.5 inches) to ensure that regular rotation occurred. In a calculation designed to illustrate the procedure developed above, x^c and x^r were derived by solving pairs of simultaneous equations with far-apart values of T. A graphical representation of the solution is given in Fig. 10 for the major surfaces, but as expected, the common correlation was not valid for the electrodes. In plotting radiation per unit area for the end plates, the exit sections were not included as these were considered to be in virtual shadow. Where appropriate, values of (ϵ/L) and C were derived from the equations given above, and these are given with other data in Table II. The values of (ϵ/L) for the shell were not found to vary much from the mean value of 0.78 ft^{-1} over the full temperature range, a value which in nearly all cases was much higher than for pure air, as indicated by the comparison shown in Table II with the fluxes calculated from the information given by Kivel and Bailey (Ref. 24). (The accuracy of this latter calculation is not, however, considered to be high owing to the extrapolation necessary for dense plasmas $(\rho/\rho' > 1)$ and to the fact that the graphical presentations in Ref. 24 are not entirely self-consistent.) It is clear from Fig. 10(a) that the radiation flux per unit area on the electrodes far exceeds the average for the shell. It is also proportional to a power of T_g greater than four. Since the contribution of ohmic heating is negligible in the case of copper electrodes, this discrepancy is ascribed to arc radiation, the presence of which invalidates the solution for the convective flux. Derived values of the convective flux have therefore not been plotted in Fig. 10(b). While Fig. 10(a) suggests that a correction can be made for the arc radiation, this was not performed in the absence of a suitable theory.

The Johns Hopkins University
APPLIED PHYSICS LABORATORY
Silver Spring, Maryland

Table II

Major Solutions

Surface	Run No.	T_t, °R	$\dot{q}$, Btu sec^{-1}	$\dot{q}^r = x^r f^r(T)$, Btu sec^{-1}	Calculated Radiation Loss (Ref. 24), Btu sec^{-1}	ϵ/L, ft^{-1}	$\dot{q}^r/A_n$, Btu $ft^{-2} sec^{-1}$	$\dot{q}^c = x^c f^c(T)$, Btu sec^{-1}	$\dot{q}^c/A_n \Delta T$, Btu sec^{-1} $ft^{-2}(°R)^{-1}$	$\dot{q}^c/A_n(\omega/\nu)^{0.8}$, Btu $ft^{-0.4} sec^{-1}$	$C = Nu(Re)^{-0.8}(Pr)^{-0.33}$
Cylindrical Section	1	4940	901	514	25	0.857	104	385	1.76×10^{-2}	0.304×10^{-2}	2.40×10^{-5}
	2	6440	1934	1482	469	-	300	552	1.54×10^{-2}	0.407×10^{-2}	-
	3	3960	671	188	544	0.694	38	483	2.83×10^{-2}	0.282×10^{-2}	2.32×10^{-5}
	4	6680	2201	1514	1570	-	307	687	2.25×10^{-2}	0.505×10^{-2}	-
	5	1600	952	5.3	0.07	0.765	1.1	947	1.72×10^{-2}	0.914×10^{-2}	2.92×10^{-5}
	6	1680	1532	5.9	0.11	0.706	1.2	1526	2.61×10^{-2}	0.117×10^{-2}	3.46×10^{-5}
	7	4240	638	261	17	0.764	53	377	2.04×10^{-2}	0.315×10^{-2}	2.94×10^{-5}
	8	5500	958	575	97	0.594	117	383	1.54×10^{-2}	0.424×10^{-2}	2.91×10^{-5}
	9	4080	568	225	10	0.764	46	343	1.94×10^{-2}	0.300×10^{-2}	2.93×10^{-5}
End Plates (2)	1	4940	538	303	16	0.892	98	235	1.71×10^{-2}	0.292×10^{-2}	0.612×10^{-5}
	2	6440	1150	875	295	-	282	274	1.49×10^{-2}	0.395×10^{-2}	-
	3	3960	443	106	342	0.746	34	337	3.14×10^{-2}	0.313×10^{-2}	0.647×10^{-5}
	4	6680	1333	858	989	-	277	477	2.49×10^{-2}	0.551×10^{-2}	-
	5	1600	510	3.7	0.04	0.868	1.1	506	14.8×10^{-2}	0.0782×10^{-2}	0.598×10^{-5}
	6	1680	699	4.0	0.07	0.865	1.3	695	18.9×10^{-2}	0.0957×10^{-2}	0.478×10^{-5}
	7	4240	320	178	11	0.955	58	142	1.22×10^{-2}	0.189×10^{-2}	0.421×10^{-5}
	8	5500	475	269	61	0.510	8.7	206	1.33×10^{-2}	0.358×10^{-2}	0.604×10^{-5}
	9	4080	297	148	6	0.922	48	149	1.34×10^{-2}	0.207×10^{-2}	0.489×10^{-5}
Electrodes (2)	1	4940	1330	763	-	-	285	567	4.79×10^{-2}	0.824×10^{-2}	0.920×10^{-5}
	2	6440	2887	2203	-	-	822	685	4.35×10^{-2}	1.14×10^{-2}	-
	3	3960	1204	265	-	-	99	939	10.20×10^{-2}	1.01×10^{-2}	1.23×10^{-5}
	4	6680	3481	2135	-	-	797	1346	8.12×10^{-2}	1.82×10^{-2}	-
	5	1600	2385	60	-	-	22	2376	77.2×10^{-2}	4.25×10^{-2}	1.79×10^{-5}
	6	1680	2977	7.5	-	-	2.8	2970	95.6×10^{-2}	4.17×10^{-2}	1.75×10^{-5}
	7	4240	940	394	-	-	147	546	3.94×10^{-2}	0.605×10^{-2}	1.09×10^{-5}
	8	5500	1372	450	-	-	168	922	6.88×10^{-2}	1.85×10^{-2}	1.79×10^{-5}
	9	4080	1095	268	-	-	100	827	8.16×10^{-2}	1.33×10^{-2}	1.70×10^{-5}

Table II (Cont'd)

Geometrical Factors

$$x^c = f^c(\dot{q}),$$

Surface	Btu $ft^{1.6} sec^{-1} (°R)^{-1}$	A_n, ft^2
Cylindrical section	0.141C	4.93
End plate	0.183C	1.55
Exit duct	0.037C	0.54
Electrode	0.277C	1.34

Chamber Volume = 2.03 ft^3.

The best correlation of end plate and cylindrical section data for the convective flux per unit area was achieved by omitting the areas of the exit ducts (although these were physically part of the end plates). Values of C were also plotted in Fig. 11 against Re, the values of Pr and k used being 0.775 and 0.516 Btu $ft^{-1} sec^{-1} (°R)^{-1}$, respectively. The values obtained for C are unusually low for such a correlation, but these depend partly on the value chosen for k (which may be too high, particularly as the surfaces concerned--and especially the electrodes--are operated at high temperatures). In addition, the values of Re may be artificially high because of the assumption that the gas vortex rotates at the same angular velocity as the arc. A refinement of values is therefore possible. Scatter in all the results reflects inaccuracies in the determination of T, ω, and $\dot{q}$, but the flow model based upon the Dittus and Boelter equation is seen to provide a basic solution for the values of the convective flux, since the major variable in ω/ν is undoubtedly ω. Therefore, except for the losses due to arc radiation, a synthesis of losses is possible.

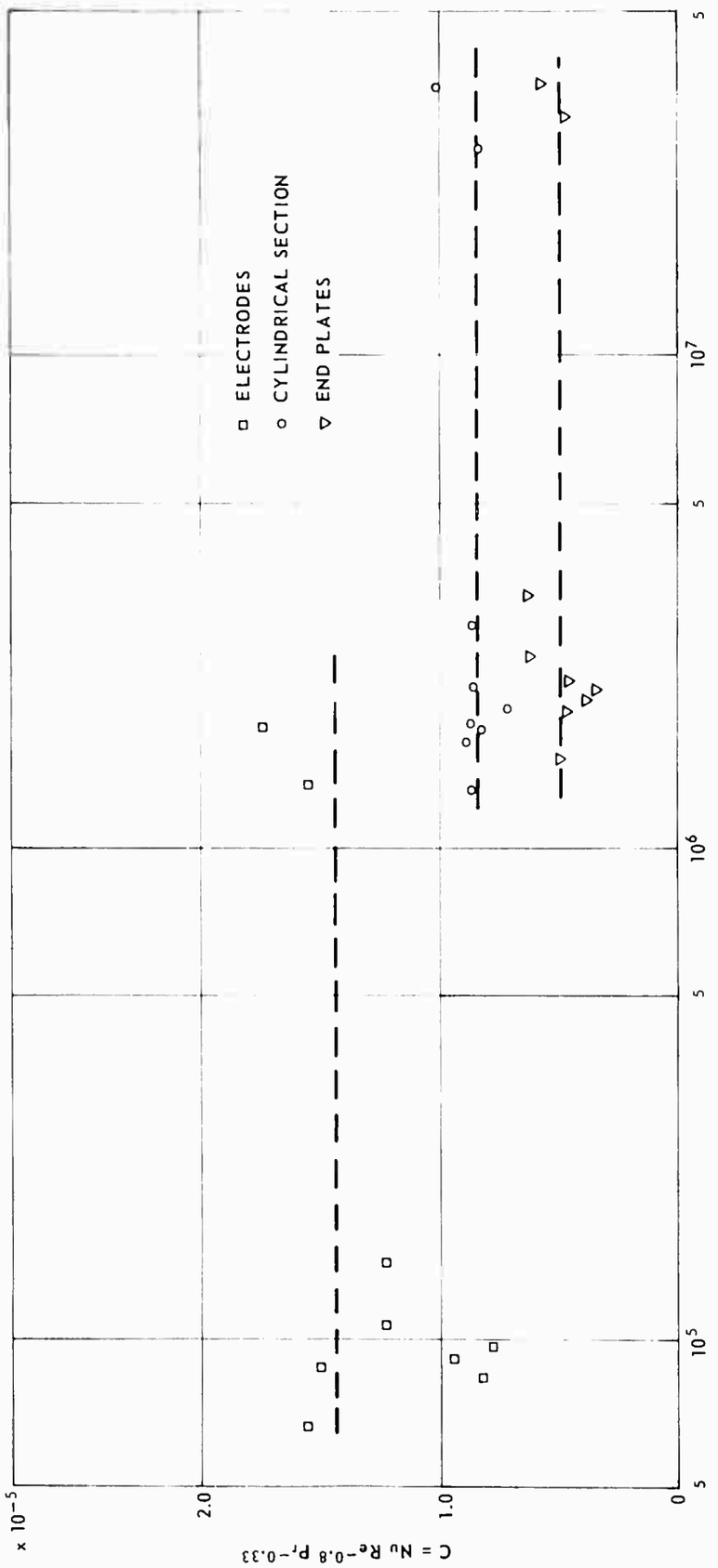

Fig. 11 $NuRe^{-0.8}\ Pr^{-0.33}$ VERSUS Re

6. CONCLUSIONS

While capable of further refinement, a satisfactory procedure has been developed for distinguishing radiative from convection losses in a split-ring type of plasma arc air heater; this in turn offers a means of optimization of efficiency. A satisfactory solution was obtained without taking arc radiation into account (the presence of which only affected the solution in the case of the electrodes). A value of gas emissivity was established that was nearly constant over the temperature range $1600 < T < 6680°R$ (the mean value of ϵ/L being $0.78\ ft^{-1}$) and that gave values for the most part much in excess of those given by tables for pure air. The excessive electrode losses were ascribed to the presence of arc radiation, which awaits a fuller theoretical treatment.

Convective losses were found to be proportional both to $(\omega/\nu)^{0.8}$ and to the temperature difference with the walls (taken as the mean difference between gas and cooling water). However, although the correlation constant $(Nu\ (Re)^{-0.8}(Pr)^{-0.33})$ was defined differently for the different surfaces, its value was unusually small--owing in all probability to the erroneous assumption that the forced vortex in the gas rotated at the same angular velocity as the arc, whereas it undoubtedly rotated more slowly. Notwithstanding this, two main conclusions were evident: (a) to keep convective losses low, the rotation rate should be limited to a value not exceeding $150\ sec^{-1}$ by suitable choice of pressure, arc gap, and arc current, the effective limit of the last being about 15 kamps (for highest efficiency, it appears that a nonrotated arc

would be best); (b) the relatively high emissivity of the copper-contaminated gas sets a practical limit on the enthalpy that may be achieved in an arc chamber of given volume and given input power. (For operation at similar power inputs but much higher enthalpies than those employed (e.g., 7000 Btu lbm^{-1}) the chamber volume would need to be reduced to a much smaller value (e.g., 0.25 ft^3).)

The Johns Hopkins University
APPLIED PHYSICS LABORATORY
Silver Spring, Maryland

ACKNOWLEDGMENTS

The author gratefully acknowledges the participation of many of his colleagues in the effort of which this was a part: in particular Dr. W. H. Avery, Dr. H. L. Olsen, Mr. S. D. Raezer, Mr. L. O. Kauffman (who operated the unit and made numerous suggestions regarding the design), Mr. R. G. Heidelbach (who supervised the design and who obtained the chrome copper forgings), Mr. G. A. Smoot (for computational assistance), and Mr. C. L. Luedeman (whose skill in welding copper made the exercise possible).

REFERENCES

1. E. A. Bunt, R. T. Cusick, L. W. Bennett, and H. L. Olsen, "Design and Operation of the Battery Power Supply of a Hypersonic Propulsion Facility," APL/JHU TG-660, February 1965 (submitted to IEEE J. of Power Apparatus and Systems).

2. L. Artsimovitch, S. Luk'ianov, I. Podgornyi, and S. Chuvatin, "Electrodynamic Acceleration of Plasma Bunches," Soviet Physics (JETP), Vol. 6, No. 1, January 1958, p. 1.

3. T. Korneff, F. Nadig, and J. Bohn, "Plasma Acceleration Experiments," Proc. of Conf. on Extremely High Temperatures, New York, Wiley, 1958, p. 197.

4. L. Fechant, "Vitesses de Déplacement d'Arcs Électriques dans l'Air," Revue Générale de l'Électricité, Vol. 68 September 1959, p. 519.

5. W. R. Warren and N. S. Diaconis, "Air Arc Simulation of Hypersonic Environments," paper presented at ARS/AFOSR International Hypersonic Conference, MIT, August 16-18, 1961 (see also H. N. Schneider and W. J. Pearce, U. S. Patent 2,964,679, December 13, 1960).

6. E. M. Winkler, R. E. Lee, and R. L. Humphrey, "Three-phase a.c. Arc Heater Studies at the Naval Ordnance Laboratory," paper presented at AGARD Specialist Meeting on "Rechauffeurs à Arc et Accélerateurs Magneto-hydrodynamiques à Usage Aérodynamique," Rhode-St Genèse, Belgium, 21-23 September 1964.

7. E. M. Winkler, R. E. Lee, R. L. Humphrey, and L. J. Milner, "The NOL 3 Megawatt Research Arc," Naval Ordnance Laboratory, NOL TR-63-114, 13 February 1964.

8. E. A. Bunt and H. L. Olsen, "Plasma Arc Heating for Hypersonic Wind Tunnels," Research 14, 353, 1961.

9. S. D. Raezer, E. A. Bunt, and H. L. Olsen, "Development of Hypersonic Propulsion Tunnels Using d.c. Plasma Arc Heating," presented at AIAA/ASME Ramjet Propulsion Conference, Naval Ordnance Laboratory, April 25, 1963 (also J. of Spacecraft and Rockets, 1, 155, 1964).

10. J. M. Reid, "High Pressure Arc Jets," ASME Paper 61-WA-246, Winter Annual Meeting, New York, 26 November 1961. *

11. E. A. Bunt, L. O. Kauffman, H. L. Olsen, and S. D. Raezer, "Discontinuous Arc Plasma Generator," Patent Serial No. 250, 722. Navy case 35108, Filed October 1, 1963.

12. E. A. Bunt and H. L. Olsen, "Overlapped Electrode for Plasma Generator," Patent Application, September 30, 1963.

13. K. Phillips, "Production and Application of Plasma Jets," AEI Engineering, January/February 1965, p. 13.

14. J. Mayersak, S. D. Raezer, and E. A. Bunt, "Confirmation of Gambill-Greene Straight-Flow Burnout Heat Flux Equation at Higher Flow Velocity," ASME J. of Heat Transfer, May 1964, p. 11.

15. R. E. Smith and R. J. Matz, "Verification of a Theoretical Method of Determining Discharge Coefficients of Venturis Operating at Critical Flow Conditions," Arnold Engineering Development Center, AEDC-TR-61-8, September 1961.

16. E. A. Bunt and H. L. Olsen, "'Pinhole Camera' for Determination of Plasma Arc Rotational Speed," ARS Journal, 31, 826, 1961.

17. J. Fabri, "Analyse des Résultats Expérimentaux Obtenus sur un Arc a Argon," paper presented at AGARD Specialist Meeting on "Rechaufferus a Arc et Accélerateurs Magneto-hydrodynamiques a Usage Aérodynamique," Rhode-St Genese, Belgium, 21-23 September 1964.

* A film illustrating split-ring arc rotation obtained at the Applied Physics Laboratory was contributed to this paper.

18. L. H. Jorgensen and G. M. Baum, "Charts for Equilibrium Flow Properties of Air in Hypervelocity Nozzles," NASA TN D-1333, September 1962.

19. W. Winovich, "On the Equilibrium Sonic-Flow Method for Evaluating Electric-Arc Air Heater Performance," NASA TN D-2132, March 1964.

20. A. Mager, "Approximate Solution of Isentropic Swirling Flow through a Nozzle," ARS Journal, 31, 1140, 1961.

21. M. Hill and J. M. Akridge, APL/JHU internal memorandum (unpublished) (also see "Transistorized Pyrometer, With and Without Feedback," APL Technical Digest, May-June 1963, p. 17.)

22. R. C. Eschenbach, D. A. Bryson, H. B. Sargent, R. J. Sarlitto and H. H. Trouve, "Characteristics of High Voltage Vortex-Stabilized Arc Heaters," IEEE Transactions on Nuclear Science, January 1964, p. 41.

23. J. K. Totten, Final Summary Technical Report on the Calendar Year 1963 Ramjet Technology Program, Section XIV, "Aerothermal Capability of Plasma Heaters," The Marquardt Corporation, June 1964.

24. B. Kivel and K. Bailey, "Tables of Radiation from High Temperature Air," AVCO Research Laboratory, Research Report 21, December 1957.

25. H. Y. Wachman, M. J. Linevsky, and J. H. McGinn, "The Effects of Electrode Contamination on the Properties of Air-Arc Plasmas," General Electric Company MSVD, R59SD427, September 21, 1959.

26. J. C. Morris, G. R. Bach, and J. M. Yos, "Research on Radiation from Arc-Heated Plasma," Aerospace Research Laboratories, ARL 64-180, October 1964.

27. T. K. Pugmire, H. E. Weber, and C. R. Marston, "Arc Heater Development for Entry Simulation," General Electric Company MSD, R63SD49, October 1963.

INITIAL DISTRIBUTION EXTERNAL TO THE APPLIED PHYSICS LABORATORY*

The work reported in TG-759 was done under Bureau of Naval Weapons Contract NOw 62-0604-c (Task Assignment P62) supported by Special Projects Office (SP-27).

ORGANIZATION	LOCATION	ATTENTION	No. of Copies
DEPARTMENT OF DEFENSE			
DDC	Alexandria, Va.		20
Department of the Navy			
Department Offices			
BuWeps	Washington, D. C.	DLI-31	2
NWSA	Washington, D. C.	R-362	1
		RMGA-81	1
		RMMP-11	1
		RMMP-21	1
Special Projects Office	Washington, D. C.	SP-22	1
		SP-27222	1
BuWepsRep	Silver Spring, Md.		1
U. S. GOVERNMENT AGENCIES			
National Aero. and Space Agy.			
Chief, Prop. Branch, Aero. Division		Mr. N. Rekos	1

*Initial distribution of this document within the Applied Physics Laboratory has been made in accordance with a list on file in the APL Technical Reports Group.

Unclassified

Security Classification

DOCUMENT CONTROL DATA - R&D

(Security classification of title, body of abstract and indexing annotation must be entered when the overall report is classified)

1 ORIGINATING ACTIVITY (Corporate author) The Johns Hopkins University, Applied Physics Lab. 8621 Georgia Avenue Silver Spring, Maryland	2a REPORT SECURITY CLASSIFICATION Unclassified 2b GROUP None

3 REPORT TITLE

Heat Transfer Effects Arising from Arc Rotation in Plasma Arc Heaters of the Self-Induced Magnetic Field Type

4 DESCRIPTIVE NOTES (Type of report and inclusive dates)

Progress Report

5 AUTHOR(S) (Last name, first name, initial)

Bunt, Edgar A.

6 REPORT DATE	7a TOTAL NO. OF PAGES	7b. NO. OF REFS
December 1965	46	27

8a. CONTRACT OR GRANT NO.	9a. ORIGINATOR'S REPORT NUMBER(S)
NOw 62-0604-c b. PROJECT NO. P62 c. d.	TG-759 9b. OTHER REPORT NO(S) (Any other numbers that may be assigned this report) None

10. AVAILABILITY/LIMITATION NOTICES

Distribution of this document is unlimited.

11. SUPPLEMENTARY NOTES	12. SPONSORING MILITARY ACTIVITY
None	Director, Special Projects Office Department of the Navy

13. ABSTRACT This paper is concerned with an analysis of the thermal behavior of high input power (~ 15 Megawatt) arc heaters operating at values of total (bulk) enthalpy up to 2500 Btu/lb. Such heaters are currently in use to supply air for aerodynamic testing purposes, including subsonic turbulent pipe flow, the operation of propulsion tunnels with "full" temperature simulation, and supersonic combustion ducts. The electrode system is essentially a "rail accelerator" adapted for continuous operation by making it re-entrant; the self-induced magnetic field brings about rapid movement of the arc roots to prevent destruction of the electrodes. The rate of rotation of the arc column (which is subject to aerodynamic drag) is shown to be a function of apparent electrode gap and current and the stagnation temperature and pressure in the arc chamber. A distinction can also be drawn between "long" and "short" arcs, depending on whether the interelectrode gap is large or small. The value of the arc rotation rate, ω (which ranges between approximately 50 and 1000 sec^{-1}) had a considerable bearing on the thermal efficiency of short-gap arcs because of the dependence of the convective losses on it. Since the chamber gases radiated much more strongly than air uncontaminated by electrode material, convective and radiative losses are distinguished by solving for first-power and fourth-power dependence on temperature difference with the walls; the convective losses are examined in conjunction with a vortex model of the gas behavior.

DD FORM 1 JAN 64 1473

Unclassified

Security Classification

14 KEY WORDS	LINK A		LINK B		LINK C	
	ROLE	WT	ROLE	WT	ROLE	WT
Arc Heater Heat Transfer Self-induced Magnetic Field Arc Rotation Rate Radiation Convection Forced Vortex Induced Vortex						

INSTRUCTIONS

1. ORIGINATING ACTIVITY: Enter the name and address of the contractor, subcontractor, grantee, Department of Defense activity or other organization *(corporate author)* issuing the report.

2a. REPORT SECURITY CLASSIFICATION: Enter the overall security classification of the report. Indicate whether "Restricted Data" is included. Marking is to be in accordance with appropriate security regulations.

2b. GROUP: Automatic downgrading is specified in DoD Directive 5200.10 and Armed Forces Industrial Manual. Enter the group number. Also, when applicable, show that optional markings have been used for Group 3 and Group 4 as authorized.

3. REPORT TITLE: Enter the complete report title in all capital letters. Titles in all cases should be unclassified. If a meaningful title cannot be selected without classification, show title classification in all capitals in parenthesis immediately following the title.

4. DESCRIPTIVE NOTES: If appropriate, enter the type of report, e.g. interim, progress, summary, annual, or final. Give the inclusive dates when a specific reporting period is covered.

5. AUTHOR(S): Enter the name(s) of author(s) as shown on or in the report. Enter last name, first name, middle initial. If military, show rank and branch of service. The name of the principal author is an absolute minimum requirement.

6. REPORT DATE: Enter the date of the report as day, month, year; or month, year. If more than one date appears on the report, use date of publication.

7a. TOTAL NUMBER OF PAGES: The total page count should follow normal pagination procedures, i.e., enter the number of pages containing information.

7b. NUMBER OF REFERENCES: Enter the total number of references cited in the report.

8a. CONTRACT OR GRANT NUMBER: If appropriate, enter the applicable number of the contract or grant under which the report was written.

8b, 8c, & 8d. PROJECT NUMBER: Enter the appropriate military department identification, such as project number, subproject number, system numbers, task number, etc.

9a. ORIGINATOR'S REPORT NUMBER(S): Enter the official report number by which the document will be identified and controlled by the originating activity. This number must be unique to this report.

9b. OTHER REPORT NUMBER(S): If the report has been assigned any other report numbers *(either by the originator or by the sponsor)*, also enter this number(s).

10. AVAILABILITY/LIMITATION NOTICES: Enter any limitations on further dissemination of the report, other than those imposed by security classification, using standard statements such as:

(1) "Qualified requesters may obtain copies of this report from DDC."

(2) "Foreign announcement and dissemination of this report by DDC is not authorized."

(3) "U. S. Government agencies may obtain copies of this report directly from DDC. Other qualified DDC users shall request through _____."

(4) "U. S. military agencies may obtain copies of this report directly from DDC. Other qualified users shall request through _____."

(5) "All distribution of this report is controlled. Qualified DDC users shall request through _____."

If the report has been furnished to the Office of Technical Services, Department of Commerce, for sale to the public, indicate this fact and enter the price, if known.

11. SUPPLEMENTARY NOTES: Use for additional explanatory notes.

12. SPONSORING MILITARY ACTIVITY: Enter the name of the departmental project office or laboratory sponsoring *(paying for)* the research and development. Include address.

13. ABSTRACT: Enter an abstract giving a brief and factual summary of the document indicative of the report, even though it may also appear elsewhere in the body of the technical report. If additional space is required, a continuation sheet shall be attached.

It is highly desirable that the abstract of classified reports be unclassified. Each paragraph of the abstract shall end with an indication of the military security classification of the information in the paragraph, represented as *(TS), (S), (C), or (U)*.

There is no limitation on the length of the abstract. However, the suggested length is from 150 to 225 words.

14. KEY WORDS: Key words are technically meaningful terms or short phrases that characterize a report and may be used as index entries for cataloging the report. Key words must be selected so that no security classification is required. Identifiers, such as equipment model designation, trade name, military project code name, geographic location, may be used as key words but will be followed by an indication of technical context. The assignment of links, rules, and weights is optional.